

Supersolidity and phase diagram of softcore bosons in a triangular lattice

Jing-Yu Gan,¹ Yu-Chuan Wen,² and Yue Yu³

¹Center for Advanced Study, Tsinghua University, Beijing, 100084, China

²Institute of Theoretical Physics and Interdisciplinary Center of Theoretical Studies,
Chinese Academy of Sciences, Beijing 100080, China

³Institute of Theoretical Physics, Chinese Academy of Sciences, Beijing 100080, China

We study the softcore extended Bose Hubbard model in a two-dimensional triangular lattice by using the quantum Monte Carlo methods. The ground state phase diagram of the system exhibits a very fruitful structure. Except the Mott insulating state, four kinds of solid states with respect to the commensurate filling factors $\rho = 1/3, 2/3$ and $\rho = 1$ are identified. Two of them (CDW II and CDW III) are newly predicted. In incommensurate fillings, superfluid, spuersolid as well as phase separation states are detected . As in the case for the hardcore bosons, a supersolid phase exists in $1/3 < \rho < 2/3$ while it is unstable towards the phase separation in $\rho < 1/3$. However, this instability is refrained in $2/3 < \rho < 1$ due to the softening of the bosons and then a supersolid phase survives.

PACS numbers: 75.10.Jm, 03.75.Lm, 05.30.Jp

Introduction A quantum matter state with non-zero order parameters characterizing both solid and superfluid phase, so-called supersolid (SS), was proposed by Penrose and Onsager fifty years ago[1]. In 1970s, it was speculated that the large zero-point quantum fluctuation in solid ^4He may induce an off-diagonal-long-range-order [2]. The recent observation of non-classical rotational inertia (NCRI) in porous Vycor or in bulk solid ^4He reported by Kim and Chan[3] have greatly revived the interest in studying this new matter state although it is still controversial whether the mechanism suggested by Refs. [2] works in explaining the NCRI [4].

Comparing to the complication of the ^4He , the di-

lute cold atom gas loaded in an optical lattice [5] is a more promising avenue to success the SS, especially when the long-range interacting atoms were already cooled to a Bose-Einstein condensate [6]. These systems may be well described by the Bose-Hubbard model [7] and its extended version. The simple Bose-Hubbard system does not allow a SS phase for the lacking of the interaction-based long range correlation. It was also checked that there is no a SS phase in the hardcore Bose-Hubbard model with a nearest neighbor repulsion in two-dimensional square lattice due to the solid-superfluid phase separation(PS), while a strip supersolid presents if the next nearest neighbor interaction is switched on [8]. The lattice frustration may stabilize a supersolid against the PS. This has been shown in the hardcore Bose-Hubbard model in a triangular lattice around the half filling [9, 10, 11, 12] whereas the supersolid order is not favored in more complicated frustrated lattices such as Kagomè lattice [13]. The next nearest neighbor interaction in triangular lattice can also lead to a strip supersolid in triangular lattice [14].

Besides the next nearest neighbor interactions and lattice frustration, softening of the on-site interaction may also stabilize the supersolid phase because more than one atoms per site are allowed, which has been confirmed either for a two-dimensional square lattice [15] or one-dimensional lattice [16].

Model and explanation to results As we have seen, the physics of the supersolid phase is determined by the interplay among the next nearest neighbor interaction, the frustration of lattice as well as the softening of the on-site interaction. In this paper, we would like to check the cooperating effect of latter two. The model we study is the extended Bose-Hubbard model in a two-dimensional triangular lattice, which reads

$$H = -t \sum_{\langle ij \rangle} (a_i^\dagger a_j + a_j^\dagger a_i) + \frac{U}{2} \sum_i n_i (n_i - 1)$$

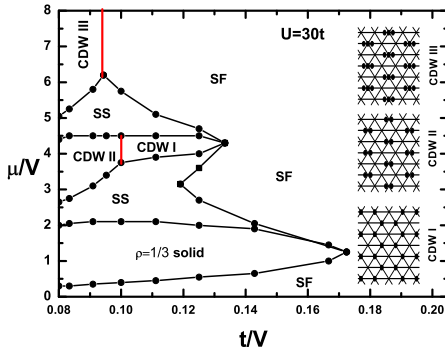


FIG. 1: (Color online) The ground state phase diagram for the extended Bose Hubbard model in the two-dimensional triangular lattice ($U = 30t$). SF is standing for the superfluid phase; MI for the Mott insulator phase. The $\rho = 1/3$ solid means one of three sets of sublattices is occupied with one atom per site. In the inset, the three different solid states are illustrated. In CDW I at $\rho = 2/3$, two sets of sublattices are occupied with one atom per site. In CDW II at $\rho = 2/3$, one set of sublattices is occupied with two atoms per site; In CDW III at $\rho = 1$, a single set of sublattices is occupied with three atoms per site.

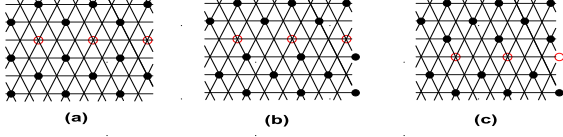


FIG. 2: (Color online) The $\rho = 1/3$ solid doped by holes. (a) Placing the doped holes into one line costs no additional potential energy; (b) shifting the lower part of the lattice introduces a domain wall without any potential energy cost; (c) the doped holes (atoms) can hop freely across the domain wall.

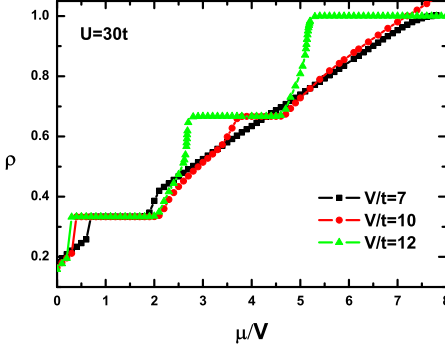


FIG. 3: (Color online) The average atom density as a function of the chemical potential for $V = 7t, 10t$ and $12t$, respectively ($U = 30t$). The system size is $L = 12$.

$$+V \sum_{\langle ij \rangle} n_i n_j - \mu \sum_i n_i, \quad (1)$$

where $a_i^\dagger(a_i)$ is the creation(annihilation) operator of bosonic atom at site i ; $n_i = a_i^\dagger a_i$ is the occupation number; μ is the chemical potential. $\langle ij \rangle$ runs over nearest neighbors. U and V represent the on-site and nearest neighbor repulsive interactions, respectively. Our central result is presented in Fig.1, the ground state phase diagram. The quantum Monte Carlo(QMC) simulation with the stochastic series expansion(SSE) [17, 18] was applied. We use t as the energy unit and focus our calculations on $U = 30t$.

This phase diagram can be qualitatively explained by strong-coupling arguments[9, 15]. When $U \rightarrow \infty$, the Hamiltonian (1) reduces to the hardcore one. The phase diagram is symmetric about $\rho = 1/2$, i.e., $\mu/V = 3$, because of the particle-hole symmetry [9]. The CDW II and CDW III as well as the upmost SS are ruled out. The phase transition from the solid to the SF is the first order one for the solid-SF PS appears at the phase boundary. Finite U breaks the particle-hole symmetry and results in other two solid phases and one more SS phase. The

phase diagram with $t = 0$ is quite easily understandable. A meaningful chemical potential is $\mu > -U/2$ otherwise $\rho \leq 0$. Raising μ , there would be several kinds of solid phases with a common commensurate wave vector $\mathbf{Q} = (4\pi/3, 0)$. The first one is the $\rho = 1/3$ solid in which one set of sublattices is occupied with single atom per site. At $\rho = 2/3$, there are two kinds of solids depending on the ratio V/U . For small values of nearest neighbor repulsion $V(V/U < 1/3)$, two sets of sublattices are occupied with single atom per site (CDW I), while for $V/U > 1/3$, one set of sublattices is occupied with two atoms per site (CDW II). For $\rho = 1$, the solid phases involved are the MI and the other one. When $V/U > 1/3$, one set of sublattices is occupied with three atoms per site (CDW III). If $V/U < 1/3$, the MI, i.e., single atom per site in the whole lattice, is the most stable. For $\rho > 1$, these commensurate solid phases are repeated in filling factors with an integer added.

Based on this strong coupling limit understanding, we can describe the phase diagram we obtained. Comparing to the hardcore boson phase diagram in ref. [9], the $\rho = 1/3$ solid lobe change slightly with only the up-bound lowered a little due to quantum fluctuations. When holes are introduced into the $\rho = 1/3$ crystal, the domain-wall proliferation mechanism, i.e., the additional holes hop freely across the domain wall, raises the kinetic energy linearly in t (see Fig. 2) and then excludes the possibility of a SS phase [9, 15]. This leads to a PS between $\rho = 1/3$ solid and a uniform superfluid with $\rho < 1/3$ [19].

When atoms are introduced into the $\rho = 1/3$ crystal, the domain-wall proliferation mechanism does not work because formation of a domain wall would cost extra potential energy. Thus, a SS phase is there right above this solid lobe, similar to that in the hardcore boson case. However, it completely separates the $\rho = 1/3$ and $\rho = 2/3$ solid lobes. Furthermore, the latter shrinks much and splits into CDW II and CDW I in the V^{-1} direction due to the ratio V/U is lowered.

Doping atoms into the $\rho = 2/3$ solid, the system behaviors differently in terms of the ratio between V and U . Following an analysis in Ref. [15] for the formation of a SS phase above the half-filling in a square lattice, we argue that a stable SS exists for $\rho > 2/3$. For $V/U < 1/3$, CDW I is doped. Since the lattice sites are either single occupied or empty, the energy cost for an additional atom fills in empty or single occupied site is $E_0^I = 6V - \mu$ or $E_1^I = U + 3V - \mu$, respectively. The energy of a single atom delocalized between these two cases is $E^I = E_0^I + \Delta^I - \sqrt{\Delta^{I2} + (6t)^2}$ with $\Delta^I = (U - 3V)/2$. Similarly, for $V/U > 1/3$, i.e., doping in CDW II, an additional atom fill either in an empty or double-occupied site. The corresponding energy cost is either $E_0^{II} = 2U - \mu$ or $E_2^{II} = 6V - \mu$, respectively. The kinetic energy of a single particle delocalized between these two cases is $E^{II} - E_0^{II} = \Delta^{II} - \sqrt{\Delta^{II2} + (6t)^2}$, with $\Delta^{II} = (3V - U)/2$. In both cases, when $\Delta \sim t$, the

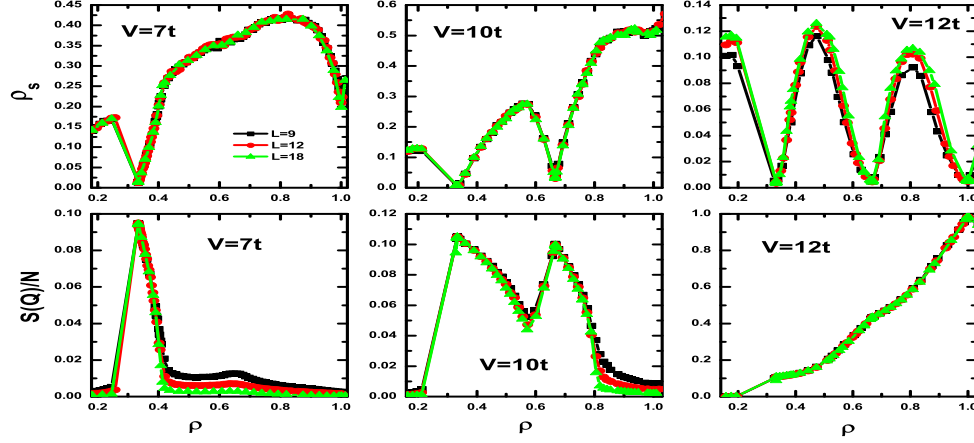


FIG. 4: (Color online) Static structure factor $S(Q)$ and superfluid density (ρ_s) as functions of atom density ρ for $V = 7t, 10t$ and $12t$, respectively ($U = 30t$). $Q = (4\pi/3, 0)$ for triangular lattice.

kinetic energy $E - E_0$ is proportional to t . Therefore, the domain wall formation was blocked and the system is stabilized against the PS [15]. As a result, these doped atoms form a SF on the top of the $\rho = 2/3$ solid background, which is thought as a SS phase. Notice that the above analysis is not applied to $U \rightarrow \infty$ because multiple occupation is not allowed. The domain wall forms if doping atoms into the $\rho = 2/3$ solid and then a PS happens [9].

For $\rho = 1$, the ground state is a solid with one set of sublattices occupied with three atoms per site (CDW III). Doping holes into this state, these additional holes move under the solid background with the effective hopping $t^* \sim t^2/(7V - 2U)$. The kinetic energy gain remains quadratic in t and small. Therefore, the SS state with $\rho > 2/3$ is stable. However, our numerical result does not fully confirm this argument as we shall see later.

Quantum Monte Carlo simulations We now portray our QMC simulations. In order to characterize different phases, we study the static structure factor $S(Q)$ with $Q = (4\pi/3, 0)$ and superfluid density ρ_s ,

$$S(Q) = \frac{1}{N} \sum_{ij} e^{iQ \cdot (r_i - r_j)} \langle n_i n_j \rangle, \quad \rho_s = \frac{\langle W^2 \rangle}{4\beta t} \quad (2)$$

where W is the winding number fluctuation of the bosonic world lines [20]; $\beta = 2L$ is the inverse of fictitious temperature and $N = L \times L$ is the lattice size. In our calculations, we use $L = 9, 12$ and 18 . A solid phase is characterized by a non-zero $S(Q)$ and $\rho_s = 0$ and a SF phase by $S(Q) = 0$ and $\rho_s \neq 0$; a SS phase is depicted by non-vanishing both of $S(Q)$ and ρ_s . Solids are categorized by their $S(Q)$ values.

Fig. 3 shows the atom density ρ varying as the chemical potential μ for $V = 7t, 10t$ and $12t$, respectively ($U = 30t$). It is seen that for each V , there is a jump from

$\rho < 1/3$ to $\rho = 1/3$ which indicates a first order phase transition. In the grand canonical ensemble, a jump in ρ is a token of a PS region. For a small V , say $V = 7t$, only $\rho = 1/3$ solid plateau is observed, i.e., there is no $\rho = 2/3$ plateau. This is different from that in the hardcore boson phase diagram for in that case there are both the $\rho = 1/3$ and $\rho = 2/3$ solid lobes symmetrically. Obviously, this is because the particle-hole symmetry is broken by the finite U . As V is raised, say $V = 10t$ and $12t$, the $\rho = 2/3$ solid plateau appears and is gradually widened. Such an observation of the $\rho = 2/3$ solid plateau indicates the shrinking of the $\rho = 2/3$ solid lobe as shown in Fig. 1. In the regions $1/3 < \rho < 2/3$ and $2/3 < \rho < 1$, both of them include a SS phase. For $V = 12t$, another solid plateau at $\rho = 1$ emerges at larger μ , while this plateau is not observed for $V = 7t$ and $10t$.

In Fig. 4, we show $S(Q)$ and ρ_s vary as functions of ρ . At $\rho = 1/3$, for all V we considered, the superfluid density $\rho_s \rightarrow 0$ while $S(Q)/N \sim 1/9$ which is an exact magnitude of the static structure factor of the $\rho = 1/3$ solid state. For $\rho > 1/3$, the results are severely dependent on the magnitude of V . For a small, say $V = 7t$, as μ increases, we observe, in turn, a $\rho = 1/3$ solid plateau, a SS phase in the region $1/3 < \rho < 0.4$ and a SF after $\rho > 0.4$. No CDW III solid state is observed at $\rho = 1$. For an intermediate value of $V (= 10t)$, both $S(Q)$ and ρ_s are finite and non-monotonous as ρ raises. A SS phase expands to the whole region from $\rho = 1/3$ to $\rho = 2/3$. At $\rho = 2/3$, $\rho_s \rightarrow 0$ while $S(Q)/N \sim 0.1$ which is the magnitude of the static structure factor of CDW I. With further increasing of ρ , there is another SS in between $2/3 < \rho < 0.8$. After $\rho = 0.8$, $S(Q) \rightarrow 0$, i.e., the system is in a pure SF phase. Again, no CDW III exists at $\rho = 1$. For large V , say $V = 12t$, $\rho_s \rightarrow 0$ at $\rho = 2/3$ while $S(Q)/N \sim 0.45$. This is CDW II solid state. As ρ increases further from $\rho = 2/3$, $S(Q)$ raises monotonously

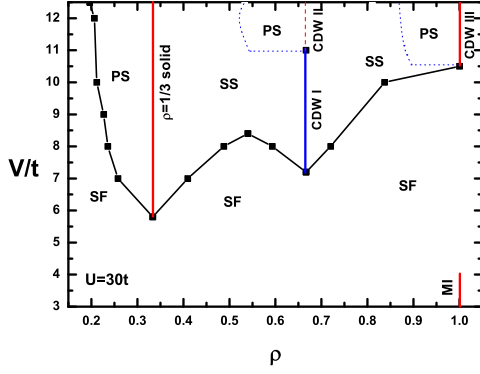


FIG. 5: (Color online) The ground state phase diagram for two-dimensional extended Bose Hubbard model in the triangular lattice in the $V - \rho$ plane at $U = 30t$.

and both ρ_s and $S(Q)$ in nonzero till $\rho = 1$. Thus, in $2/3 < \rho < 1$, the ground state is a SS phase. At $\rho = 1$, the ground state is another kind of solid state with $\rho_s \rightarrow 0$ and $S(Q)/N \sim 1$, i.e., CDW III.

Phase diagrams and conclusions We scan V from $3t$ to $12t$ with a wider step. This sketches the ground state phase diagram of the system. Fig. 1 and Fig. 5 are its projections to the $\mu - V^{-1}$ and $V - \rho$ planes, respectively. The PS phase is explicitly shown in Fig. 5 and its width grows as V is strengthened. On the left hand sides of the CDW II and CDW III in Fig. 5, we use dot lines labelling two possible PS regions. These PS states are neither supported by our early analysis nor confirmed by our numerical data. However, our data could not exclude these PS. What we see is although there seems no discontinuity in ρ of μ , e.g., for $V = 12t$ in Fig. 3, the change of ρ may be very sharp and for some specific magnitudes of V it is near a right-angle. We squint towards there are no these PS states but simulations with larger lattice size and lower fictitious temperature are required and confirmations with other numerical methods, e.g., a canonical ensemble calculation, are necessary. No such an ambiguity for the hardcore bosons because there are no CDW II and CDW III states [9].

At $\rho = 1$, for quite small values of V , say $V = 3t$ and $4t$, the MI phase ($\rho_s \rightarrow 0$ and $S(Q) \rightarrow 0$) exists. There is a SF region in between the MI and CDW III solid states and this region is suppressed as U becomes strong. Comparing with the hardcore boson phase diagram depicted in Ref. [9], we see that the softcore phase diagram is much more fruitful. And on the other hand, it is more practical to be verified by experiments because U is always finite. Comparing with the softcore bosons in a square lattice [15], the frustration of a triangular lattice opens a wider window to explore the SS state. The CDW III solid state at integer filling as the counterpart of the MI state is another new feature in the present model and is worth to be experimentally measured. Mermin-

Wagner theorem obstructs the various phases described in the present work to be detected in any finite temperature. However, it may become possible if we trap the atoms by an additional shallow trapping potential as the Bose-Einstein condensate is observed in a trapped two-dimensional cold Bose atom gas.

This work was supported in part by Chinese National Natural Science Foundation.

-
- [1] N. Penrose and L. Onsager, Phys. Rev. **104**, 576 (1956)
 - [2] A. F. Andreev and I. M. Lifshitz, Sov. Phys. JETP **29**, 1107 (1969); G. Chester, Phys. Rev. A **2**, 256 (1970); A. J. Leggett, Phys. Rev. Lett. **25**, 1543 (1970).
 - [3] E. Kim and M. H. W. Chan, Nature **427**, 225 (2004); Science **305**, 1941 (2004).
 - [4] D. M. Ceperley, B. Bernu, Phys. Rev. Lett. **93**, 155303 (2004); N. Prokofev, B. Svistunov, ibid. **94**, 155302 (2005); D. E. Galli, M. Rossi, L. Reatto, Phys. Rev. B **71**, 140506(R) (2005).
 - [5] M. Greiner, I. Bloch, O. Mandel, T. W. Hansch, and T. Esslinger, Phys. Rev. Lett. **87**, 160405 (2001). C. Orzel, A. K. Tuchman, M. L. Fenslau, M. Yasuda, and M. A. Kasevich, Science **291**, 2386 (2001). M. Greiner, O. Mandel, T. Esslinger, T. W. Hansch and I. Bloch, Nature **415**, 39 (2002). M. Greiner, O. Mandel, T. Esslinger, T. W. Hansch and I. Bloch, Nature **419**, 51 (2002).
 - [6] A. Griesmaier, J. Werner, S. Hensler, J. Stuhler, and T. Pfau, Phys. Rev. Lett. **94**, 160401 (2005).
 - [7] D. Jaksch, C. Bruder, J. I. Cirac, C. W. Gardiner and P. Zoller, Phys. Rev. Lett. **81**, 3108 (1998).
 - [8] G. G. Batouni and R. T. Scalettar, Phys. Rev. Lett. **84**, 1599 (2000);
 - [9] S. Wessel and M. Troyer, Phys. Rev. Lett. **95**, 127205 (2005).
 - [10] D. Heidarian and K. Damle, Phys. Rev. Lett. **95**, 127206 (2005).
 - [11] R. G. Melko, A. Paramekanti, A. A. Burkov, A. Vishwanath, D. N. Sheng, and L. Balents, Phys. Rev. Lett. **95**, 127207 (2005).
 - [12] M. Boninsegni and N. Prokofev, Phys. Rev. Lett. **95**, 237204 (2005).
 - [13] S. V. Isakov, S. Wessel, R. G. Melko, K. Sengupta, and Yong Baek Kim, E-preprint, cond-mat/0602430.
 - [14] R. G. Melko, A. Del Maestro, and A. A. Burkov, cond-mat/0607501
 - [15] P. Sengupta, L. P. Pryadko, F. Alet, M. Troyer, and G. Schmid, Phys. Rev. Lett. **94**, 207202 (2005).
 - [16] G. G. Batrouni, F. Hébert, and R. T. Scalettar, E-preprint, cond-mat/0605518.
 - [17] A. W. Sandvik and J. Kurkijärvi, Phys. Rev. B **43**, 5950 (1991); A. W. Sandvik, J. Phys. A **25**, 3667 (1992); A. W. Sandvik, R. R. P. Singh, and D. K. Campbell, Phys. Rev. B **56**, 14510 (1997).
 - [18] A. W. Sandvik, Phys. Rev. B **59** R14157701 (1999); O. f. Syljuasen and A. W. Sandvik, Phys. Rev. E **66**, 046701 (2002).
 - [19] N. G. Zhang and C. L. Henley, Phys. Rev. B **68**, 14506 (2003).
 - [20] E. L. Pollock and D. M. Ceperley, Phys. Rev. B **36**, 8348 (1987).